

Lipopenia and Skin Barrier Abnormalities in DGAT2-deficient Mice*

Received for publication, October 6, 2003, and in revised form, December 10, 2003
Published, JBC Papers in Press, December 10, 2003, DOI 10.1074/jbc.M311000200

Scot J. Stone^{‡§}, Heather M. Myers[‡], Steven M. Watkins[¶], Barbara E. Brown^{||},
Kenneth R. Feingold^{||**‡§§}, Peter M. Elias^{||**}, and Robert V. Farese, Jr.^{‡§‡¶¶}

From the [‡]Gladstone Institute of Cardiovascular Disease, San Francisco, California 94141-1900, the [§]Cardiovascular Research Institute and Departments of ^{**}Dermatology and ^{‡‡}Medicine, University of California, San Francisco, California 94143, the Departments of ^{§§}Medicine and ^{¶¶}Dermatology and Medical Service, Veterans Affairs Medical Center, San Francisco, California 94121, and ^{¶¶}Lipomics Technologies, West Sacramento, California 95691

The synthesis of triglycerides is catalyzed by two known acyl-CoA:diacylglycerol acyltransferase (DGAT) enzymes. Although they catalyze the same biochemical reaction, these enzymes share no sequence homology, and their relative functions are poorly understood. Gene knockout studies in mice have revealed that DGAT1 contributes to triglyceride synthesis in tissues and plays an important role in regulating energy metabolism but is not essential for life. Here we show that DGAT2 plays a fundamental role in mammalian triglyceride synthesis and is required for survival. DGAT2-deficient (*Dgat2*^{-/-}) mice are lipopenic and die soon after birth, apparently from profound reductions in substrates for energy metabolism and from impaired permeability barrier function in the skin. DGAT1 was unable to compensate for the absence of DGAT2, supporting the hypothesis that the two enzymes play fundamentally different roles in mammalian triglyceride metabolism.

Triglycerides (triacylglycerols) are the major storage form of energy in eukaryotic organisms. However, excessive deposition of triglycerides in white adipose tissue (WAT)¹ leads to obesity and in non-adipose tissues (such as pancreatic β cells, skeletal muscle, and liver) is associated with tissue dysfunction referred to as lipotoxicity (1, 2). Therefore, an understanding of the processes that mediate triglyceride synthesis is of significant biomedical importance.

Triglycerides are synthesized from diacylglycerol and activated forms of fatty acids (fatty acyl-CoAs) in a reaction catalyzed by acyl-CoA:diacylglycerol acyltransferase (DGAT) enzymes (3–5). The genes for two DGAT enzymes, DGAT1 and DGAT2, have been identified (6, 7). Both DGAT1 and DGAT2 are ubiquitously expressed, with the highest levels of expression found in tissues that are active in triglyceride synthesis, such as WAT, small intestine, liver, and mammary gland (6, 7). Both enzymes are intrinsic membrane proteins, although DGAT1 has 6–12 putative transmembrane domains, whereas DGAT2 has one. Both also have similarly broad fatty acyl-CoA

substrate specificities in *in vitro* assays (7). However, despite their ability to catalyze similar reactions, DGAT1 and DGAT2 belong to different gene families that share neither DNA nor protein sequence similarity. DGAT1 is homologous to the acyl-CoA:cholesterol acyltransferase enzymes, ACAT1 and ACAT2, which are involved in cholesterol ester biosynthesis (6), whereas DGAT2 shares homology with acyl-CoA:monoacylglycerol acyltransferase enzymes (8–13). This raises the question of why two different types of DGAT enzymes have emerged from convergent evolution.

Insights into the functions of DGAT1 and DGAT2 in triglyceride metabolism have been provided by studies in yeast. Through deletion and overexpression studies, several groups have demonstrated that *DGA1*, the yeast homologue of DGAT2, is the major DGAT enzyme contributing to triglyceride synthesis and storage in yeast (14–16). In contrast, *ARE2*, a yeast homologue of DGAT1, plays a minor role in triglyceride synthesis. Interestingly, mutant *Saccharomyces cerevisiae* strains devoid of DGAT activity and lacking triglycerides are viable and grow normally, indicating that triglycerides are not essential for the survival of this yeast. However, a recent study showed that triglyceride synthesis is essential for viability of the fission yeast *Schizosaccharomyces pombe* (17).

To determine the physiological functions of DGAT1 and DGAT2 in mammalian triglyceride metabolism, we used gene knockout approaches in mice. Mice lacking DGAT1 (*Dgat1*^{-/-} mice) are viable and have reduced triglycerides in tissues, including WAT (18, 19). *Dgat1*^{-/-} mice are resistant to diet-induced obesity through a mechanism involving increased energy expenditure (18) and also exhibit increased sensitivity to leptin and insulin (19, 20). These findings indicate that DGAT1 plays an important role in the regulation of energy metabolism. However, the effects of DGAT1 deficiency on triglyceride metabolism in general are not profound. For example, plasma triglyceride levels in *Dgat1*^{-/-} mice are normal, and significant amounts of triglycerides are present in their tissues, including WAT. These findings suggest that other triglyceride-synthesizing enzymes participate in energy homeostasis.

To understand the role of DGAT2 in triglyceride synthesis and energy homeostasis, we generated *Dgat2*^{-/-} mice. Our results indicate that DGAT2 is the DGAT responsible for the majority of triglyceride synthesis in mice and provide significant insights into the functional differences between DGAT1 and DGAT2.

MATERIALS AND METHODS

Generation of Stable DGAT1- and DGAT2-expressing Cell Lines—McArdle rat hepatoma (McA-RH7777) cells from the American Type Culture Collection were cultured in Dulbecco's modified Eagle's medium with 10% fetal bovine serum and 10% horse serum in a 37 °C incubator with 5% CO₂. Mouse DGAT1 and DGAT2 with N-terminal FLAG epitopes (MGDYKDDDDG, epitope underlined) were cloned into

* This work was supported by a postdoctoral fellowship from the Canadian Institutes of Health Research (to S. J. S.) and National Institutes of Health Grant DK56084 (to R. V. F.). The costs of publication of this article were defrayed in part by the payment of page charges. This article must therefore be hereby marked "advertisement" in accordance with 18 U.S.C. Section 1734 solely to indicate this fact.

¶¶ To whom correspondence should be addressed. E-mail: rfarese@gladstone.ucsf.edu.

¹ The abbreviations used are: WAT, white adipose tissue; DGAT, acyl-CoA:diacylglycerol acyltransferase; BAT, brown adipose tissue; PBS, phosphate-buffered saline; C/EPB α , CCAAT/enhancer-binding protein; E, embryonic day.

TABLE I
Real-time PCR primer sequences

Gene	Sense	Antisense
DGAT-2	5'-AGTGGCAATGCTATCATCATCGT-3'	5'-AAGGAATAAGTGGGAACCAGATCA-3'
DGAT-1	5'-TTCCGCCTCTGGGCATT-3'	5'-AGAATCGGCCACAATCCA-3'
UCP-1	5'-ACACCTGCCTCTCTCGGAAA-3'	5'-TAGGCTGCCAATGAACACT-3'
Insulin-like growth factor-binding protein 18 S	5'-TGGACAGCTTCCACCTGATG-3'	5'-TTTCTTGAGGTCGGCGATCT-3'
Phosphoenolpyruvate carboxykinase	5'-AGTCCCTGCCCTTGTACACA-3'	5'-GATCCGAGGGCCCTCACTAAAC-3'
Glucose-6-phosphatase	5'-CCACAGCTGCTGCAGAAC-3'	5'-GAAGGGTCCGATGGCAA-3'
Fructose-1,6-bisphosphatase	5'-CCATGCAAAGGACTAGGAACA-3'	5'-TACCAGGGCCGATGTCAAC-3'
Sterol regulatory-binding protein 1c	5'-TGGCAGCCGGGTATGC-3'	5'-TCCATGGCAAGGACCAACA-3'
Acetyl-CoA carboxylase-1	5'-GGCCCCGGGAAGTCACTGT-3'	5'-GGAGCCATGGATTGCACATT-3'
Fatty acid synthase	5'-GAATCTCATTGGCTTACGATGAG-3'	5'-CAATGGCCCCGATGT-3'
Stearoyl-CoA desaturase 1	5'-GCTGCGGAACTTCAGGAAAT-3'	5'-AGAGACGTGCTACTCTGGACTT-3'
	5'-CCTTCCCCTTCGACTACTCTG-3'	5'-GCCATGCAGTCGATGAAGAA-3'

eukaryotic expression vector pCDNA3.1 (Invitrogen, Carlsbad, CA). For transfections, 1 μ g of pcDNA3.1 expression vector containing DGAT1, DGAT2, or LacZ was incubated with 3 μ l of FuGENE 6 transfection reagent (Roche Diagnostics) for 20 min, and the mixture was added to a 60-mm culture dish containing 2 ml of medium and cells at ~50% confluence. After 48 h, transfected cells were split 1:4 and cultured in growth medium containing 600 μ g/ml G418 to generate G418-resistant colonies. Cell lines stably expressing DGAT1 and DGAT2 were identified by immunoblotting of cell lysates with an anti-FLAG M2 monoclonal antibody (Sigma) followed by detection with SuperSignal West Pico Detection kit (Pierce).

Generation of DGAT2-deficient Mice—DGAT2 genomic fragments were amplified by PCR from 129/SvJae mouse genomic DNA with primers derived from the mouse DGAT2 cDNA sequence. A replacement type targeting vector was constructed in pN1KloxP (a gift from Joachim Herz, University of Texas, Dallas, TX) by subcloning a ~1-kb short arm containing sequences upstream of exon 3 and a ~5-kb long arm containing sequences downstream of exon 4. This construct was used to produce DGAT2-targeted 129/SvJae embryonic stem cells, which were then used to generate mice carrying the mutation. The disruption of the *Dgat2* gene was confirmed by Southern blotting of genomic DNA digested with EcoRI and a probe located upstream of the vector sequences (described in Fig. 2a). *Dgat2*^{-/-} mice for use in this study were generated by intercrossing *Dgat2*^{+/-} mice of mixed genetic background (50% C57BL/6J and 129/SvJae). *Dgat2*^{+/-} mice were also crossed with transgenic mice that constitutively express Cre recombinase (21) to remove *neo* from the allele. *Dgat2*^{-/-} mice lacking the *neo* gene had the same phenotype as *Dgat2*^{-/-} mice with *neo*.

Mice were housed in a pathogen-free barrier facility (12 h light/12 h dark cycle) and fed a standard chow diet. All experiments were approved by the Committee on Animal Research of the University of California, San Francisco.

Gene Expression Analyses—Total RNA was extracted from tissues (RNA STAT, Tel-Test, Friendswood, TX), and samples (1 μ g) were reverse-transcribed into cDNA with oligo(dT)₁₂₋₁₈ and Superscript II reverse transcriptase (Invitrogen). Each 30- μ l PCR contained 1 μ l of cDNA, 15 μ l of 2 \times QuantiTect SYBR green master mixture (Qiagen, Valencia, CA), 10 pmol each of forward and reverse primer, and 0.5 μ l of 1 μ M fluorescein. Real-time PCR was performed and analyzed with the iCycler real-time PCR detection system (Bio-Rad). Expression levels were normalized to 18 S ribosomal RNA. Primer pairs for specific genes are listed in Table I.

For skin analysis, full thickness skin was removed, the subcutaneous fat was scraped away, and the sample was immersed dermis-side down in 10 mM EDTA in phosphate-buffered saline (PBS) (Ca²⁺ and Mg²⁺ free) for 45 min at 37 °C. The skin was then chilled on ice and the epidermis was quickly peeled away from the dermis. Both tissues were immediately snap frozen in liquid nitrogen and stored at -80 °C until RNA was extracted.

DGAT Activity Assays—Liver and brown adipose tissue from newborn mice were separately homogenized in 50 mM Tris-HCl (pH 7.4) and 250 mM sucrose by 10 strokes of a Potter-Elvehjem tissue homogenizer. Cell debris and nuclei were pelleted by centrifugation at 600 \times g for 5 min. The supernatant (10–50 μ g of protein) was used for *in vitro* DGAT activity assays, performed as described (7), with either 20 or 100 mM MgCl₂ in the assay buffer.

Blood Chemistries—Plasma triglyceride and free fatty acid concentrations were measured with colorimetric kit assays (Triglycerides GPO and Free Fatty Half-Micro Test, Roche Diagnostics). Plasma glucose levels were determined with a glucometer (Accu-chek, Roche Diagnostics).

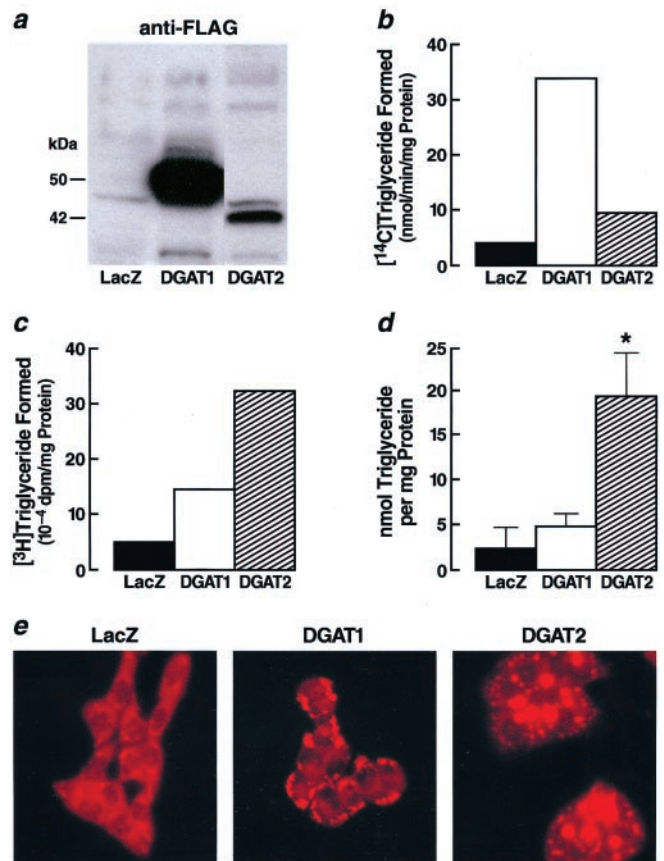


FIG. 1. Overexpression of DGAT1 and DGAT2 in McArdle RH7777 cells. Cells were transfected with vectors containing LacZ, FLAG-tagged mouse DGAT1, or FLAG-tagged mouse DGAT2 cDNA. *a*, immunoblot demonstrating stably transfected clones expressing DGAT1 and DGAT2. Cellular lysates were analyzed by immunoblotting with an anti-FLAG antibody. *b*, increased *in vitro* DGAT activity in cellular lysates of DGAT1- and DGAT2-transfected cells. Results are from a representative experiment; the experiment was repeated twice with similar results. *c*, increased triglyceride synthesis in intact cells expressing DGAT2. Transfected cells expressing DGAT1 and DGAT2 were incubated in Dulbecco's modified Eagle's medium containing 10% fetal bovine serum, 10% horse serum, and 10 μ Ci of [³H]glycerol for 6 h. Total lipids were extracted and separated by TLC, and the radioactivity in the triglyceride band was quantified. Results are from a representative experiment; the experiment was repeated twice with similar results. *d*, increased triglyceride storage in intact cells expressing DGAT2. Total lipids were extracted from cells expressing DGAT1 and DGAT2 and separated by TLC, and the triglyceride band was quantified. *, *p* < 0.05 (*n* = 3). *e*, Nile Red staining of neutral lipids in DGAT1- and DGAT2-transfected cells. Note the small lipid droplets around the cell periphery in DGAT1-expressing cells and the numerous large cytosolic lipid droplets in DGAT2-expressing cells.

Lipid Analyses—Lipids were extracted from total carcass or tissue homogenates in ClCH₃:MeOH (2:1) and separated by thin-layer chromatography with the solvent system hexane:ethyl ether:acetic acid

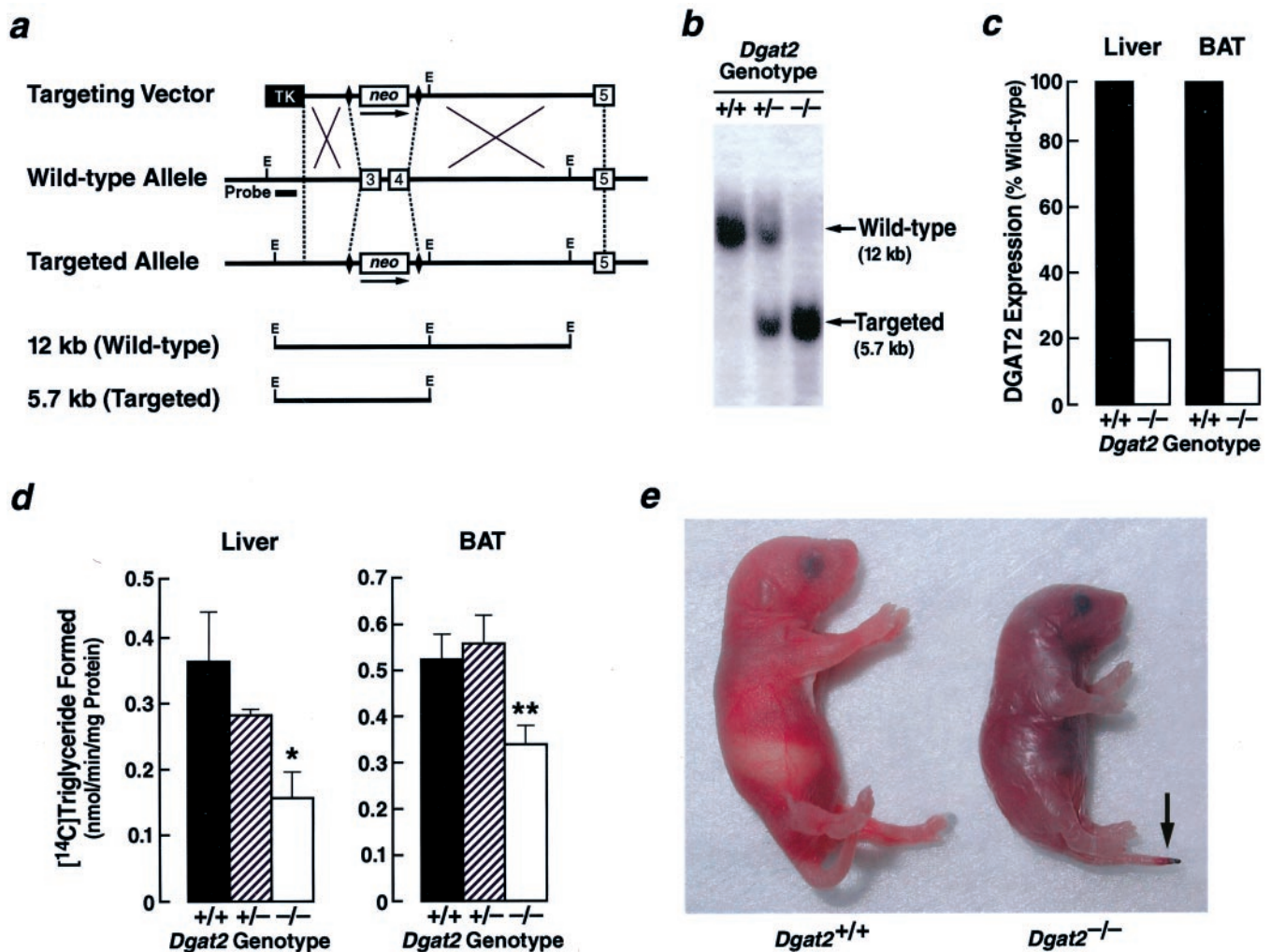


FIG. 2. Generation of *Dgat2*^{-/-} mice. *a*, gene-targeting strategy. Homologous recombination of the targeting vector with *Dgat2* replaces ~700 bp of sequences with a *neo* gene and deletes exons 3 and 4. The targeted allele is identified by a 6-kb decrease in an EcoRI restriction fragment that is detected by a ~500-bp probe located upstream of the targeting vector. The probe was generated by PCR amplification of genomic DNA (primers: 5'-TGCTCAGCAGGTAGCTCATCT-3' and 5'-GCAGATAGTACATTGTCCGAC-3'). Black diamonds indicate LoxP sites. *b*, Southern blot demonstrating the generation of *Dgat2*^{+/-} and *Dgat2*^{-/-} mice. *c*, decreased DGAT2 mRNA expression in *Dgat2*^{-/-} liver and BAT. DGAT2 mRNA was quantified by real-time PCR as described under "Materials and Methods." *d*, reduced DGAT activity in tissues of *Dgat2*^{-/-} mice. Tissue homogenates from liver and BAT of wild-type, *Dgat2*^{+/-}, and *Dgat2*^{-/-} mice ($n = 3$) were assayed for the incorporation of [¹⁴C]oleoyl-CoA into triglycerides. *, $p < 0.05$ versus wild-type; **, $p < 0.001$ versus wild-type. *e*, gross appearance of *Dgat2*^{-/-} mice. Note the smaller size, shiny skin, absent milk stripe, and necrotic tail (arrow).

(80:20:1) on Silica Gel G-60 TLC plates. Lipids were visualized by exposure to iodine vapor or charred by dipping the plate into a solution of 10% cupric sulfate and 8% phosphoric acid and heating to 180 °C. Triglyceride mass was quantified by the method of Snyder and Stephens (22) with triolein as a standard. To visualize neutral lipid droplets in intact cells, cells were fixed in 1.5% glutaraldehyde in PBS for 5 min and then stained with 0.1 μg/ml Nile Red in acetone for 5 min. Cells were then washed twice with PBS, and coverslips were mounted with a drop of PBS. Fluorescence was visualized with fluorescein isothiocyanate optics.

For compositional analyses, lipids were extracted from newborn mouse carcasses, plasma, and skin and from milk produced by DGAT2-heterozygote females. Methyl esters of milk and carcass triglycerides and plasma lipids were analyzed by gas-liquid chromatography as described (19).

In other experiments, the composition of lipids in the plasma and liver was determined by high-throughput methods developed by Lipomics. The lipids from plasma (200 μl) and liver (25 mg) were extracted with chloroform:methanol (2:1, v/v) in the presence of authentic internal standards by the method of Folch *et al.* (23). Individual lipid classes within the extract were separated by preparative TLC as described by Watkins *et al.* (24). Isolated lipid classes were trans-esterified in 3 N methanolic HCl in a sealed vial under a nitrogen atmosphere at 100 °C for 45 min. The resulting fatty acid methyl esters were extracted with hexane containing 0.05% butylated hydroxytoluene and prepared for

gas chromatography by sealing the hexane extracts under nitrogen. Fatty acid methyl esters were separated and quantified by capillary gas chromatography using a gas chromatograph (Hewlett-Packard model 6890, Wilmington, DE) equipped with a 30-m DB-225MS capillary column (J&W Scientific, Folsom, CA) and a flame-ionization detector as described (24).

Acylceramide levels in skin lipids were measured by TLC after lipid extraction (25). The following one-dimensional, high-performance TLC systems provided optimal separation and quantification of ceramide and glucosylceramide species for subsequent scanning densitometry: (i) chloroform:methanol:water (40:10:1, v/v) to 2 and 5 cm, successively; (ii) chloroform:methanol:acetic acid (94:4:1.5, v/v) to the top; and (iii) *n*-hexane:diethylether:acetic acid (65:35:1, v/v). After final development, the plates were dried, cooled, dipped in charring solution (1.5% cupric sulfate in acetic acid:sulfuric acid:orthophosphoric acid:water (50:10:10:30, v/v)), and charred at 160 °C for 15 min. Lipids were quantified with a CAMAG scanning densitometer (CAMAG Scientific, Wilmington, NC) (26).

Triglyceride Synthesis in Intact Liver Cells—Livers were removed from newborn mice, cut into small pieces, and incubated at 37 °C for 15 min in 5 ml of 2% collagenase (Sigma) and 1% bovine serum albumin in Krebs-Ringer phosphate buffer. Cells were washed twice with 10 ml of Dulbecco's modified Eagle's medium, 10% fetal bovine serum, resuspended in 5 ml of medium, and plated in a 60-mm culture dish. Cell viability was 80–90% as assessed by staining with trypan blue. After

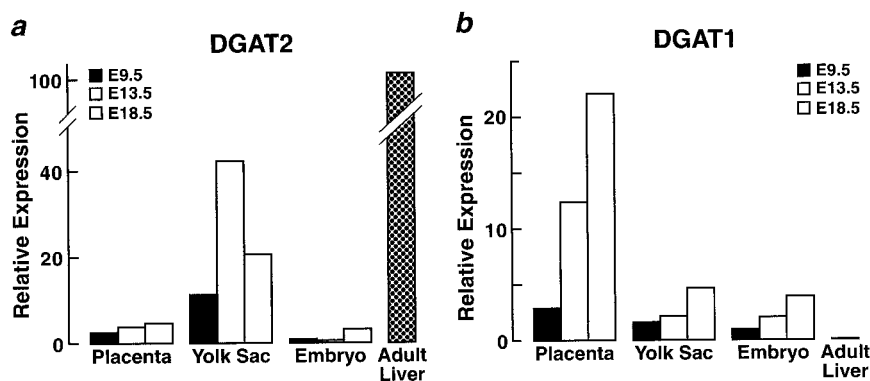
TABLE II
Gene expression in newborn *Dgat2*^{-/-} mice

For all measurements, *n* = 4–8 mice, except UCP-1, where *n* = 5–7 mice. See text for abbreviations.

Category	Gene	Tissue	Expression relative to wild-type	<i>p</i>
<i>arbitrary units</i>				
Fetal nutrition	Insulin-like growth factor-binding protein 1	Liver	1.7	<0.05
Gluconeogenesis	Phosphoenol pyruvate carboxykinase	Liver	1.3	NS ^a
	Glu-6-Pase	Liver	1.7	NS
	Fru-1,6-BP	Liver	0.4	NS
Fatty acid synthesis	ACC-1	Liver	0.4	NS
	Fatty acid synthase	Liver	1.0	NS
	Stearoyl-CoA desaturase 1	Liver	1.3	NS
	ACC-1	BAT	1.2	NS
	Stearoyl-CoA desaturase 1	BAT	1.3	NS
Thermogenesis	UCP-1	BAT	0.5	0.06

^a NS, not significant.

FIG. 3. Expression of DGAT2 (a) and DGAT1 (b) in embryonic tissues. mRNA expression levels in placenta, yolk sac, and embryos at E9.5, E13.5, and E18.5 were quantified by real-time PCR. Expression levels were obtained from pooled cDNA from three mice, and the results were normalized to 18 S ribosomal RNA. The experiment was repeated once with similar results.



2 h, 1 ml of fresh medium containing 10 μ Ci of [³H]glycerol \pm 0.5 mM oleate, 0.5% bovine serum albumin was added, and cells were incubated at 37 °C in 5% CO₂ overnight. Lipids were then extracted from cells and separated by TLC, and the incorporation of radiolabel into triglyceride and phospholipid was determined.

Histological Analyses—Newborn mice were fixed in 4% paraformaldehyde in PBS overnight, embedded in paraffin, cut into sections, and stained with hematoxylin and eosin. To visualize neutral lipids in liver and brown adipose tissue (BAT), tissues were snap-frozen in OCT and isopentane, sectioned, and stained with Oil Red O. For ultrastructural studies, skin biopsy and scale samples were minced into 1-mm³ pieces and fixed overnight (16 h) at 4 °C in 2% glutaraldehyde and 2% paraformaldehyde with 0.06% calcium chloride in 0.1 M sodium cacodylate buffer (pH 7.3). Specimens were then placed in 0.1 M sodium cacodylate buffer at 4 °C until further processing. Portions of each tissue sample were then placed in either 0.2% ruthenium tetroxide or 1.5% osmium tetroxide (Polysciences, Warrington, PA) with 1.5% potassium ferrocyanide in 0.1 M sodium cacodylate (pH 7.4), at room temperature in the dark for 45 min (27, 28). After rinsing with buffer, tissue samples were dehydrated in a graded ethanol series, and subsequently embedded in a low viscosity, epoxy resin containing DER 736 and Epon 812. Thin sections were stained with lead citrate and/or uranyl acetate and examined with a Zeiss 10A electron microscope (Zeiss, Thornville, NY) operating at 60 kV.

Liver Glycogen—Livers were digested with 5 N KOH and treated with saturated sodium sulfate and ethanol to isolate glycogen granules. Samples were boiled in 2 N HCl and neutralized with 4 N KOH and 0.1 M triethylamine to release glucose. Glycogen-derived glucose was measured with a plasma glucose assay kit (Sigma 115-A).

Skin Barrier Function Assays—Newborn mice were rinsed in PBS and successively dehydrated in 25, 50, 75, and 100% methanol for 1 min each. Mice were then rehydrated with PBS and stained in 0.1% toluidine blue in PBS for 10 min, destained with PBS for 20 min, and then photographed. All steps were at room temperature. Transepidermal water loss was measured with an electrolytic water analyzer (MEECO, Warrington, PA) (29). Because mice were housed in different locations, two different instruments were used to measure water loss from newborn mice and mice that received skin grafts. These instruments had different sensitivities, providing different ranges of absolute transepidermal water loss measurements. Skin surface temperature was measured with a digital thermometer (model 4600; Yellow Springs Instruments, Yellow Springs, OH).

Mouse Skin Grafts—Full-thickness skin pieces (~1 cm²) were obtained from newborn wild-type and *Dgat2*^{-/-} pups and placed in Dulbecco's modified Eagle's medium. Wild-type and *Dgat2*^{-/-} skin was grafted onto the left and right sides of athymic nude mice (Jackson Laboratory, Bar Harbor, ME), respectively, onto a wound created by removing a similar-sized piece of full-thickness skin. Wound edges were sutured and mice were allowed to recover. Mouse chow was supplemented with tablets (SCID's MD, Bio-Serv, Frenchtown, NJ) containing sulfamethoxazole (60 mg/tablet) and trimethoprim (10 mg/tablet). Three weeks after transplantation, fur was removed from the grafts and transepidermal water loss was measured as described above.

Statistical Analyses—Data are presented as mean \pm S.D. unless otherwise indicated. For parametric data, means were compared by *t* test or by analysis of variance followed by the Student-Newman-Keuls test. For nonparametric data, the Mann-Whitney rank-sum test or Kruskal-Wallis test was used.

RESULTS

Overexpression of DGAT2 Promotes Triglyceride Storage in Cultured Cells—To examine the roles of DGAT1 and DGAT2 in cellular triglyceride metabolism, we overexpressed FLAG-tagged mouse DGAT1 (~50-kDa) and DGAT2 (~42-kDa) in McA-RH7777 cells. In these stably transfected cell lines, DGAT1 protein levels were considerably higher than DGAT2 levels (Fig. 1a). This was reflected by DGAT activity levels, as measured by *in vitro* assays, which were 11- and 3-fold higher in DGAT1- and DGAT2-overexpressing cells, respectively, than in LacZ-transfected control cells (Fig. 1b). However, triglyceride synthesis measured by the incorporation of [³H]glycerol into triglyceride in cells was 2-fold higher in DGAT2- than in DGAT1-overexpressing cells (Fig. 1c). Additionally, the intracellular triglyceride mass was 4-fold higher in DGAT2- than in DGAT1-overexpressing cells (Fig. 1d). In DGAT2-transfected cells, the intracellular triglyceride accumulated in large cytosolic lipid droplets (Fig. 1e). In DGAT1-transfected cells, lipid droplets were also present but considerably smaller. These results suggested that DGAT2 activity potently contributes to the synthesis and storage of intracellular triglycerides.

Generation of DGAT2-deficient Mice—To test the role of DGAT2 in triglyceride synthesis and storage *in vivo*, we generated *Dgat2*^{-/-} mice. A gene-targeting vector was designed to replace exons 3 and 4 of murine *Dgat2*, regions that are highly conserved in DGAT2 gene family members, with *neo* (Fig. 2a). This vector was used to generate embryonic stem cells and, subsequently, mice carrying the targeted allele. Homozygous disruption of *Dgat2* in mice was demonstrated by Southern blotting of mouse genomic DNA (Fig. 2b). DGAT2 mRNA expression in BAT and livers of newborn *Dgat2*^{-/-} mice was reduced by 80–90% (Fig. 2c). The residual *Dgat2* mRNA in *Dgat2*^{-/-} tissues was nonfunctional. Amplification and sequencing of the transcript showed that exons 3 and 4 were deleted, resulting in the introduction of a premature stop codon. A protein produced from this allele would be severely truncated (112 amino acids instead of 387) with 29 novel amino acids. DGAT activity was reduced by 53 and 35% in *Dgat2*^{-/-} liver and BAT homogenates, respectively, when the *in vitro* assay mixture contained 20 mM MgCl₂ (Fig. 2d). The lesser reduction in DGAT activity in BAT may reflect higher expression of murine *Dgat1* in BAT than in liver.² No reduction in DGAT activity was found in *Dgat2*^{-/-} liver and BAT when the assay mixture contained 100 mM MgCl₂, a condition that selectively measures DGAT1 activity (7) (not shown). DGAT activity levels in tissues of wild-type and *Dgat2*^{+/-} mice were similar in assays using 20 mM MgCl₂.

Triglyceride Synthesis by DGAT2 Is Essential for Energy Homeostasis—Offspring from heterozygote intercrosses were found in the expected Mendelian distribution (wild-type, *n* = 14; *Dgat2*^{+/-}, *n* = 29; *Dgat2*^{-/-}, *n* = 14; *p* = 0.999 by χ^2 test). Although *Dgat2*^{+/-} mice were healthy and indistinguishable from wild-type mice, *Dgat2*^{-/-} mice were smaller (Fig. 2e), rarely suckled, and died 2–24 h after birth. Necrosis of the tail developed in *Dgat2*^{-/-} mice that survived for 8–24 h.

Newborn *Dgat2*^{-/-} mice weighed 20% less (1.13 ± 0.12 versus 1.41 ± 0.14 g, *n* = 16–18, *p* < 0.001) and were 15% shorter (2.5 ± 0.11 versus 2.9 ± 0.09 mm, *n* = 3–5, *p* < 0.001) than wild-type littermates, suggesting intrauterine growth retardation. Fetal *Dgat2*^{-/-} mice had a 14% reduction in body weight at embryonic day (E) 18.5 (0.97 ± 0.09 versus 1.13 ± 0.08 g for wild-type embryos, *n* = 4, *p* = 0.04). At E12.5, there was no difference in the size of wild-type and *Dgat2*^{-/-} embryos, indicating that growth retardation occurred later in development. Levels of mRNA expression of insulin-like growth factor-binding protein 1, a marker of intrauterine fetal nutrition whose levels are inversely correlated with birth weight (30), were increased 1.7-fold in livers of *Dgat2*^{-/-} newborn mice (Table II).

To explore the role of DGAT enzymes in mouse embryonic development, we examined the expression levels of DGAT2 and DGAT1 in yolk sac, placenta, and embryos at E9.5, E13.5, and E18.5. Whereas DGAT1 expression was highest in the placenta, DGAT2 was expressed at the highest level in the yolk sac (Fig. 3, a and b). At E12.5, *Dgat2*^{-/-} embryos had an 86% reduction in tissue triglycerides (not shown), suggesting that DGAT2 deficiency results in a defect in the ability of embryos to synthesize and store triglycerides at or before this stage of fetal development.

To investigate the early postnatal lethality of *Dgat2*^{-/-} mice, we examined their substrates for energy metabolism. The plasma levels of triglycerides, free fatty acids, and glucose were 70–90% lower in newborn *Dgat2*^{-/-} mice (Fig. 4, a–c) than in *Dgat2*^{+/-} and wild-type mice. Plasma glucose levels were also reduced by 68% in E18.5 *Dgat2*^{-/-} embryos (Fig. 4c). Hepatic glycogen levels were similar in wild-type and *Dgat2*^{-/-} em-

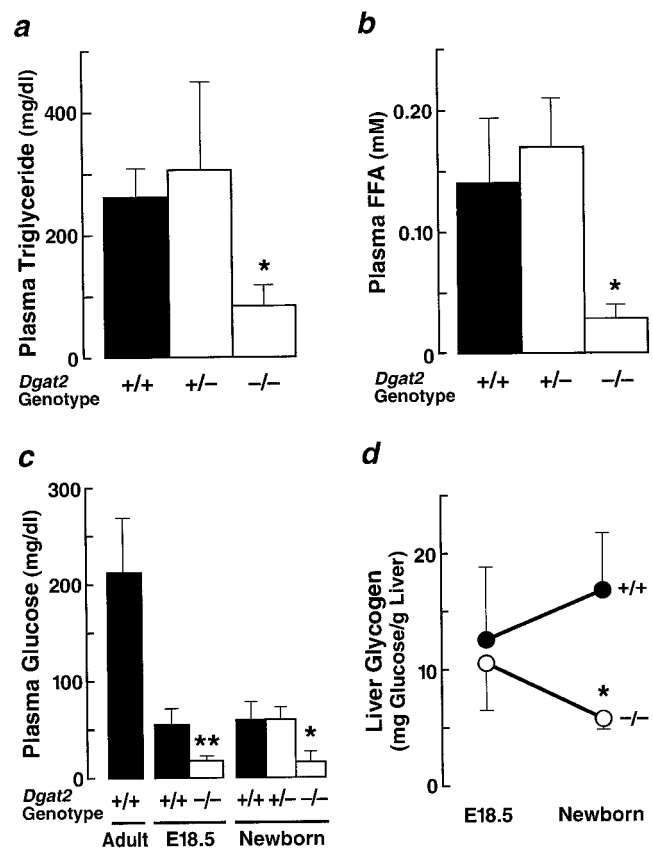


FIG. 4. Effects of DGAT2 deficiency on circulating sources of energy and liver glycogen stores. a, reduced plasma triglyceride levels in *Dgat2*^{-/-} mice (*n* = 3–9/group). *, *p* < 0.05 versus wild-type. b, reduced plasma free fatty acid (FFA) levels in *Dgat2*^{-/-} mice (*n* = 3–9/group). *, *p* < 0.05 versus wild-type. c, hypoglycemia in E18.5 embryos and newborn *Dgat2*^{-/-} mice (*n* = 5–14/group). *, *p* < 0.001 versus newborn wild-type mice. **, *p* < 0.05 versus fetal wild-type mice. d, depletion of liver glycogen after birth in *Dgat2*^{-/-} newborn mice (*n* = 3–4/group). *, *p* < 0.05 versus wild-type mice.

bryos at E18.5, but differed in newborn mice (Fig. 4d). After birth, hepatic glycogen levels increased in wild-type mice, likely because of the nutrition provided by suckling, but decreased in *Dgat2*^{-/-} mice after birth and were 67% lower than those of wild-type mice. We attempted to rescue the *Dgat2*^{-/-} pups by repeated subcutaneous injections of glucose in saline. However, this prolonged their lives only for a few hours.

To exclude the possibility that the hypoglycemia in newborn *Dgat2*^{-/-} mice resulted from impaired gluconeogenesis, we examined the expression levels of three key gluconeogenic enzymes (phosphoenolpyruvate carboxykinase, glucose-6-phosphatase, and fructose-1,6-bisphosphatase). No significant differences were found in the expression levels of these genes in livers from newborn wild-type and *Dgat2*^{-/-} mice (Table II).

Total carcass triglyceride content of *Dgat2*^{-/-} mice was reduced by 93% (Fig. 5a) with no change in carcass protein content (33.7 ± 3.4 versus 30.8 ± 1.9 mg of protein/g body weight, *p* = 0.362). Most of the triglyceride in *Dgat2*^{-/-} mice was present in BAT (~67%), although triglyceride content was reduced by more than 60% in this tissue (Fig. 5b). In livers of fetal and newborn *Dgat2*^{-/-} mice, triglycerides were nearly undetectable (Fig. 5c). Cholesterol ester and free fatty acid levels also were reduced in *Dgat2*^{-/-} carcass and liver (Fig. 5, a and c); the phospholipid content was unchanged. Oil Red O staining of histological sections revealed a dramatic reduction in neutral lipid content in *Dgat2*^{-/-} liver and a marked reduction in BAT (Fig. 6).

There was no difference in the weight of brown fat pads of

² S. Stone, unpublished results.

FIG. 5. Reduced triglyceride content in carcass (a), BAT (b), and liver (c) of *Dgat2*^{-/-} mice. Lipids were extracted from tissues and separated by TLC. Triglyceride content was quantified and normalized to body or tissue weight. For carcasses, data are for three wild-type and two *Dgat2*^{-/-} mice; *, $p = 0.006$ versus wild-type mice. For BAT, $n = 4-7$ /group; **, $p < 0.001$ versus wild-type mice. For livers, $n = 3-6$ /group; ***, $p < 0.05$ versus wild-type mice. The TLC plate for liver shows lipids for newborn mice. The triglyceride content of liver and BAT of *Dgat2*^{+/-} mice was similar to that of wild-type mice (not shown). CE, cholesterol esters; TG, triglycerides; FFA, free fatty acids; DAG, diacylglycerol; PL, phospholipids.

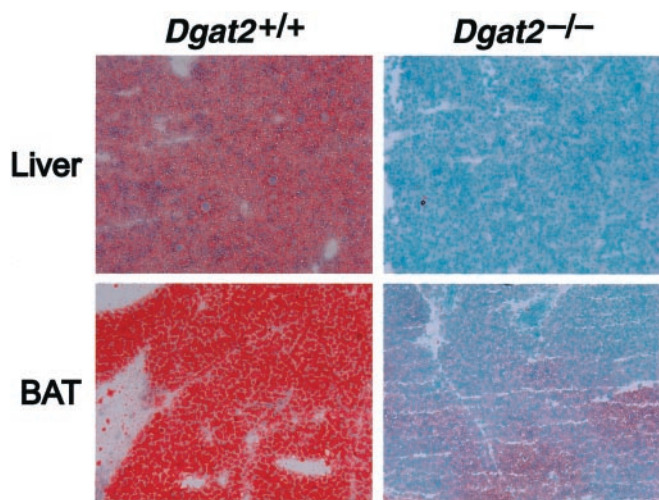
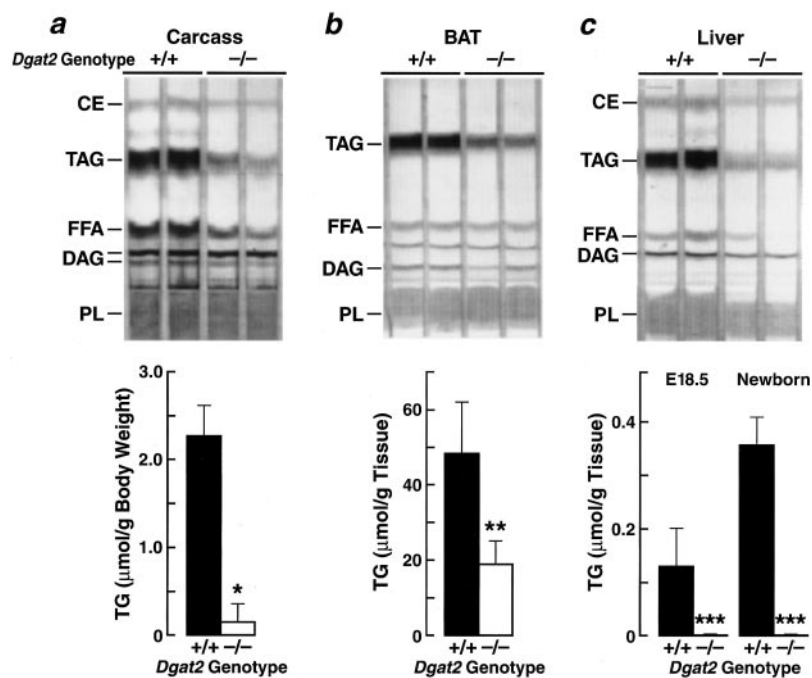


FIG. 6. Reduced content of neutral lipids in liver and BAT of *Dgat2*^{-/-} mice. Sections of liver and BAT were stained with Oil Red O.

newborn wild-type and *Dgat2*^{-/-} mice (9.38 ± 1.8 versus 10.4 ± 1.8 mg of BAT/g body weight, $p = 0.196$), and histological analysis of sections of BAT showed no obvious abnormalities. The mRNA expression of the uncoupling protein 1 gene was reduced by 50% in *Dgat2*^{-/-} mice (Table II). The reductions in BAT fatty acid content and uncoupling protein 1 gene expression suggested a reduced capacity for thermogenesis. Indeed, the surface body temperature was markedly lower in *Dgat2*^{-/-} mice than in wild-type mice (24.4 ± 0.3 versus 27.3 ± 0.7 °C, $n = 4-9$, $p < 0.001$).

The profound reductions in tissue and plasma triglycerides in *Dgat2*^{-/-} mice prompted us to examine the expression levels of genes involved in lipogenesis. The expression levels of sterol regulatory element binding protein-1c, fatty acid synthase, and acetyl-CoA carboxylase-1 in newborn liver and BAT were not significantly different in wild-type and *Dgat2*^{-/-} mice (Table II), indicating that the reduced triglyceride levels were unlikely to be caused by defective expression of genes involved in fatty acid biosynthesis.

Analysis of the fatty acid composition of liver triglycerides showed that all fatty acid classes were reduced by >95% in

livers from *Dgat2*^{-/-} mice (Fig. 7a).³ There were no significant differences in phospholipid fatty acid composition (not shown). The content of linoleic acid (18:2), an essential fatty acid provided in the diet, was virtually undetectable in triglycerides in the livers and plasma of *Dgat2*^{-/-} mice (Fig. 7b). Additionally, the content of linoleic acid in free fatty acids in both liver and plasma was greatly reduced (77 and 85%, respectively). Linoleic acid was also reduced by ~60% in cholesterol esters in the liver. In pregnant *Dgat2*^{+/-} mice, the linoleic acid content was not different in fatty acids of plasma and milk triglycerides (not shown), indicating that the essential fatty acid deficiency of *Dgat2*^{-/-} mice did not result from insufficient maternal supply. In addition, phospholipids of livers of wild-type and *Dgat2*^{-/-} mice had similar levels of linoleic acid, suggesting that the transfer of essential fatty acids to other lipid classes in the embryo was normal (Fig. 7b).

The profound reduction in tissue triglycerides in *Dgat2*^{-/-} mice indicated that DGAT1 is unable to compensate for DGAT2 deficiency. The mRNA expression level of DGAT1 was similar in livers of wild-type and *Dgat2*^{-/-} mice (Fig. 8a), apparently accounting for the significant residual DGAT activity observed in *Dgat2*^{-/-} liver (Fig. 2d). We hypothesized that DGAT1 was unable to compensate for DGAT2 because of reduced substrate availability. Indeed, primary hepatocytes isolated from newborn *Dgat2*^{-/-} mice were capable of incorporating [³H]glycerol into triglyceride at levels that were 50–60% of those in wild-type hepatocytes, and this capacity was stimulated by the addition of 0.5 mM oleate to the cell culture medium (Fig. 8b). The incorporation of [³H]glycerol into phospholipids by *Dgat2*^{-/-} hepatocytes was similar to that of wild-type hepatocytes, whereas incorporation into diacylglycerol was reduced by 37% (not shown).

DGAT2 Is Essential for Permeability Barrier Function of the Skin—Newborn *Dgat2*^{-/-} mice were easily recognized by the appearance of their skin, which lacked elasticity and was shinier than that of wild-type mice (Fig. 2e). Within a few hours after birth, the skin of *Dgat2*^{-/-} mice appeared dry and cracked. In contrast to newborn wild-type mice that were not suckling, *Dgat2*^{-/-} mice rapidly lost weight, suggesting dehydration because of increased transepidermal water loss (Fig. 9a). Indeed, transepidermal water loss in newborn wild-type

FIG. 7. Altered composition of fatty acids in liver triglycerides of *Dgat2*^{-/-} mice. *a*, reduced content of all fatty acids in liver triglycerides from *Dgat2*^{-/-} newborn mice. *p* < 0.05 versus wild-type mice for all fatty acids. *b*, reduced content of linoleic acid in liver triglycerides (TG), cholesterol esters (CE), and free fatty acids (FFA), and in plasma triglycerides and free fatty acids of *Dgat2*^{-/-} mice. For livers, *n* = 3/genotype. Plasma triglyceride and free fatty acid data was from plasma pooled from five mice. *, *p* < 0.05 versus wild-type mice. PC, phosphatidylcholine.

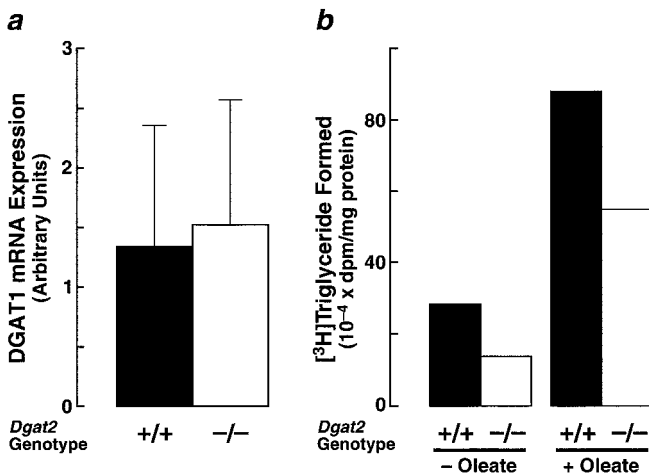
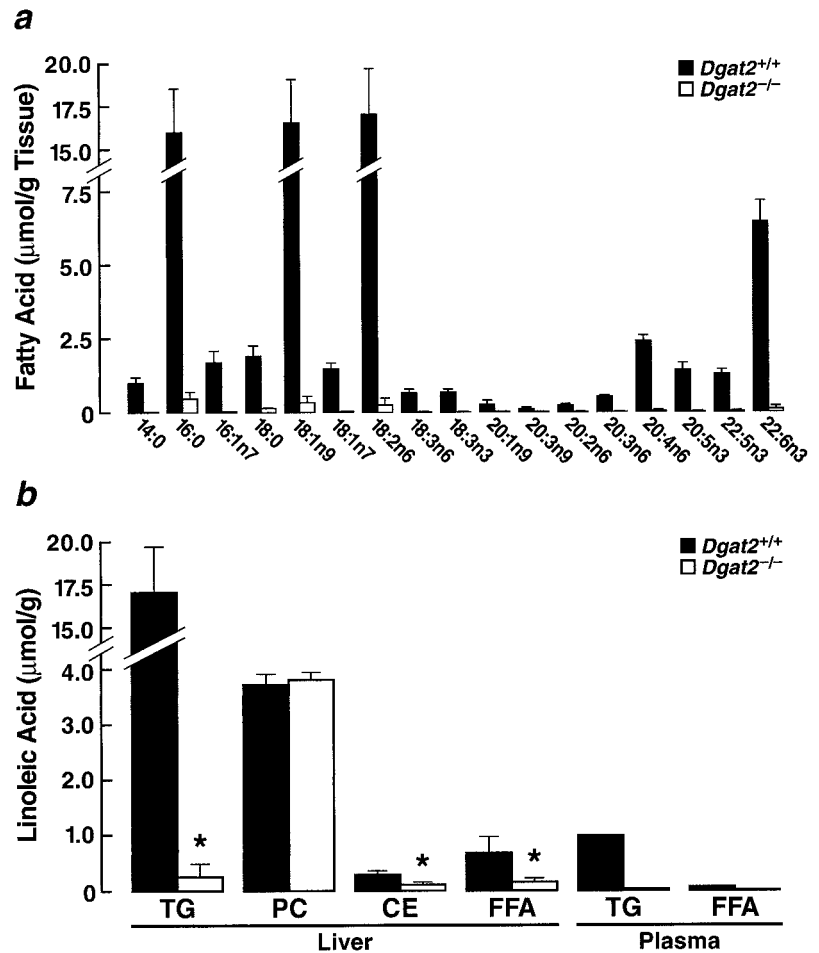


FIG. 8. Triglyceride synthesis in primary hepatocytes from *Dgat2*^{-/-} mice. *a*, normal DGAT1 expression in livers of *Dgat2*^{-/-} mice. DGAT1 mRNA was quantified by real-time PCR as described under "Materials and Methods" (*n* = 6–7/genotype). *b*, primary hepatocytes of *Dgat2*^{-/-} mice are capable of synthesizing triglycerides in the absence or presence of oleate. Primary liver cells were isolated from collagenase-digested livers of newborn wild-type and *Dgat2*^{-/-} mice. Cells were plated in 60-mm dishes and incubated for 18 h with 10 μCi of [³H]glycerol and 0.5 mM oleate, 0.5% bovine serum albumin. The incorporation of [³H]glycerol into triglyceride was determined by liquid scintillation counting and normalized to cellular protein. The experiment was repeated once with similar results.

mice was 0.06 mg/cm²/h ± 0.01 (*n* = 3), whereas it was 0.24 mg/cm²/h in a single *Dgat2*^{-/-} newborn, indicative of impaired permeability barrier function in the latter (31, 32). The barrier abnormality in *Dgat2*^{-/-} mice was also demonstrated by in-

creased permeation of toluidine blue dye (33) (Fig. 9*b*). Subcutaneous injections of saline combined with increasing the ambient humidity from 50 to 85% prolonged the life of *Dgat2*^{-/-} mice for several hours, indicating that the cutaneous barrier abnormality contributed to the early demise of these animals.

Examination of sections of neonatal *Dgat2*^{-/-} skin by light microscopy revealed consistent abnormalities, including compact orthohyperkeratosis of affected stratum corneum, thinning of the epidermis, and effacement of the epidermal rete ridges/papillary projections, leading to a flattened dermo-epidermal interface (Fig. 9*c*). Evidence of abnormal epidermal differentiation was not observed. To further assess the structural basis for the permeability abnormality in *Dgat2*^{-/-} skin, we examined the lamellar secretory system by electron microscopy (Fig. 10). Although the numbers of lamellar bodies in the epidermis were normal, *Dgat2*^{-/-} epidermis had reduced numbers of lamellar membranes in the stratum corneum extracellular spaces compared with wild-type epidermis (Figs. 10, *A* and *B*). In addition, the individual lamellar bodies often lacked normal contents (Fig. 10, *C* and *D*). Because of the decreased lamellar contents, secreted material at the stratum granulosum-stratum corneum interface exhibited small amounts of loosely organized lamellae (Fig. 10*E*). These results indicate that the barrier abnormality in the *Dgat2*^{-/-} epidermis results from abnormalities in the lamellar body secretory system.

To determine whether DGAT2 is normally expressed in neonatal skin, we examined DGAT2 and DGAT1 mRNA expression in the epidermis and dermis from a 1-day-old wild-type mouse. DGAT2 mRNA was expressed at much higher levels in the epidermis than in the dermis (Fig. 11). DGAT1, which is highly expressed in adult sebaceous glands (34), was nearly

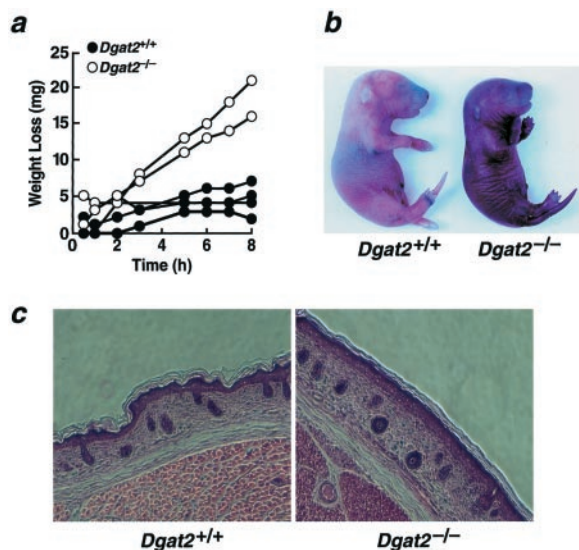


FIG. 9. Abnormal appearance and skin defects in newborn *Dgat2*^{-/-} mice. *a*, rapid weight loss in nonsuckling newborn *Dgat2*^{-/-} mice. Newborn mice were isolated from mothers, and body weights were measured over time. The increased weight loss in *Dgat2*^{-/-} mice is presumably because of water loss. *b*, increased toluidine blue staining of newborn *Dgat2*^{-/-} mice. Mice were immersed in toluidine blue for 10 min, rinsed with PBS, and photographed. *c*, sections of skin of newborn mice stained with hematoxylin and eosin.

undetectable in both the epidermis and dermis of neonatal skin.

The lipids of *Dgat2*^{-/-} neonatal skin exhibited a 96% reduction in triglyceride content (Fig. 12*a*). Other lipids in *Dgat2*^{-/-} skin were similar to those of wild-type skin. Analysis of the composition of the lipids of *Dgat2*^{-/-} skin revealed marked reductions in the linoleic acid content of triglycerides and free fatty acids, and a moderate reduction in phosphatidylcholine (Fig. 12*b*). Furthermore, the content of acylceramide, a skin lipid that contains linoleic acid and is thought to be a significant determinant of skin permeability (35), was reduced by more than 60% (1.05 ± 0.02 versus $2.89 \pm 0.11\%$ of total skin lipids, $n = 3$ per genotype, $p < 0.0001$).

To determine whether the barrier abnormality of the *Dgat2*^{-/-} epidermis was because of the absence of DGAT2 in the skin, wild-type and *Dgat2*^{-/-} skin was grafted onto athymic nude mice. Three weeks after transplantation, both wild-type and *Dgat2*^{-/-} skin grafts developed hair that was normal in appearance (Fig. 13*a*). Additionally, transepidermal water loss from wild-type and *Dgat2*^{-/-} transplanted skin was similar (Fig. 13*b*), indicating that the skin barrier abnormalities of *Dgat2*-deficient mice could be corrected by restoring DGAT2 function to the non-skin tissues.

DISCUSSION

Previous murine gene knockout studies demonstrated that DGAT1 plays a major role in modulating signals of energy homeostasis but a lesser role in bulk triglyceride synthesis (19, 20, 36, 37). In this study, we show that DGAT2 plays a comparatively greater role in basal triglyceride synthesis and storage and that DGAT2 deficiency is incompatible with survival. Mice lacking DGAT2 are lipopenic, with severely reduced triglyceride content in their tissues. As a result, they die in the early postnatal period, apparently from abnormalities in energy and skin homeostasis. Thus, our results suggest that the two DGAT enzymes have fundamentally different *in vivo* functions.

Severe reductions in energy substrates appear to account in part for the early postnatal lethality of *Dgat2*^{-/-} mice. Plasma

glucose, triglyceride, and free fatty acid levels were decreased by 70–90%, liver glycogen was reduced by 67%, and carcass triglycerides were almost undetectable. Because newborn mice have virtually no WAT, they are dependent on obtaining energy supplies from maternal milk. However, *Dgat2*^{-/-} mice did not suckle, probably because of their dehydration, restrictive skin, hypothermia, and energy deficiency. Therefore, they appear to be incapable of increasing stores of energy and rapidly consume their available glycogen and fatty acids.

The energy metabolism aspects of the phenotype resemble those found in mice lacking CCAAT/enhancer-binding protein α (C/EBP α) (38). The lack of C/EBP α results in the absence of WAT and defective gluconeogenesis, because of a defect in the transcription of genes for gluconeogenic enzymes. As a result, these mice have reduced hepatic glycogen levels and hypoglycemia and die soon after birth. However, there are differences in the phenotypes of C/EBP α -deficient and *Dgat2*^{-/-} mice. First, genes involved in gluconeogenesis are expressed normally in *Dgat2*^{-/-} mice. Second, skin abnormalities were not reported for C/EBP α -deficient mice. Finally, whereas C/EBP α -deficient mice are characterized by lipodystrophy and therefore reduced ability to store triglycerides in adipose tissue, *Dgat2*^{-/-} mice exhibit a near total absence of triglycerides in all tissues. This difference is also illustrated in other mouse models of lipodystrophy (e.g. A-ZIP/F (39) and sterol response element-binding protein 1c (40) transgenic mice), which are generally viable, even though they lack triglycerides in WAT. These lipodystrophic mice accumulate large amounts of triglycerides in their livers, whereas *Dgat2*^{-/-} mice do not.

The intrauterine growth defect observed in *Dgat2*^{-/-} mice suggests a role for DGAT2 in mouse embryonic nutrition. The expression level of insulin-like growth factor-binding protein 1 in the livers of fetal *Dgat2*^{-/-} mice (E18.5) was increased, indicating that their nutritional state had been compromised (30). Because *Dgat2*^{-/-} embryos at E12.5 were normal in size, growth retardation does not appear to occur until after E12.5. At E13.5, relatively high levels of DGAT2 expression were observed in the yolk sac, an organ that plays a major role in the nutrition of mouse embryos during early developmental stages (41–43). Thus, triglyceride synthesis by DGAT2 in the yolk sac may play a role in fetal nutrition in mice.

DGAT1 was unable to compensate for the absence of DGAT2, despite its presence in *Dgat2*^{-/-} tissues (such as the liver and BAT). However, *Dgat2*^{-/-} hepatocytes were capable of synthesizing triglycerides when fatty acid substrates were provided. This result suggests that the lack of compensation by DGAT1 relates to insufficient substrate availability for the enzyme. We speculate that the utilization of fatty acids for oxidative metabolism precludes them from reaching sufficient concentrations to activate triglyceride synthesis by DGAT1. DGAT1 and DGAT2 may also play fundamentally different roles in the cell, and fatty acids in the livers of *Dgat2*^{-/-} mice may not gain access to the DGAT1 enzyme. Indeed, intracellular lipid droplets in McArdle cells overexpressing DGAT1 and DGAT2 appeared to have different cellular distributions, suggesting that DGAT1 and DGAT2 might reside in different subcellular compartments.

Severe skin abnormalities also contributed to the postnatal lethality of *Dgat2*^{-/-} mice. The skin was abnormal in appearance and exhibited defective permeability barrier function. As a result, the mice became rapidly dehydrated, which likely contributed to their demise. The defective cutaneous barrier in *Dgat2*^{-/-} mice was unexpected, and its etiology is incompletely understood. We suspect that it relates to alterations in skin lipid metabolism. The epidermal lipids had reduced levels of acylceramide, a key lipid thought to be involved in barrier

FIG. 10. Abnormalities in the lamellar body secretory system in *Dgat2*^{-/-} epidermis. *Dgat2*^{-/-} epidermis exhibited reduced numbers of lamellar membranes in the stratum corneum extracellular spaces (A, arrows) compared with wild-type epidermis (B), reduced lamellar body contents (C, arrowheads) compared with wild-type epidermis (D), and abnormalities in the secreted contents at the stratum granulosum-stratum corneum interface (E, arrow). A, B, D, and E, ruthenium tetroxide staining post-fixation; C, osmium tetroxide staining post-fixation. Bar is 0.25 μ m.

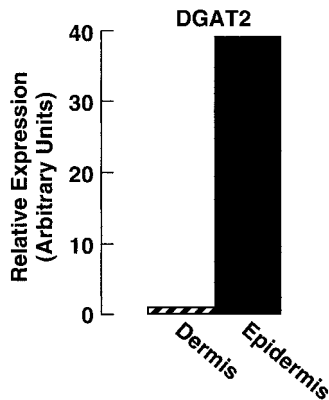
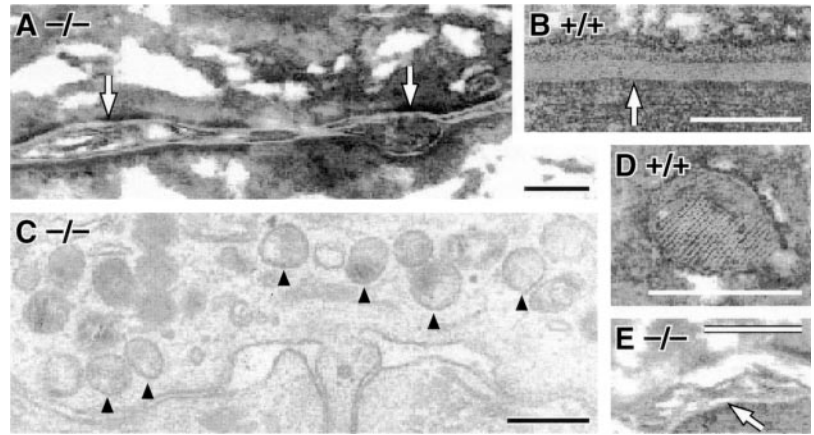


FIG. 11. Expression of DGAT2 mRNA in neonatal skin. Skin from a wild-type newborn mouse was separated into epidermis and dermis, and the expression of DGAT2 mRNA was measured by real-time PCR.

maintenance (35), and ultrastructural analyses revealed abnormal lamellar membranes in the stratum corneum. The lamellar membranes are derived from lamellar bodies, whose formation requires the appropriate lipids (fatty acids, cholesterol, and glucosylceramide) in the stratum granulosum.

Some aspects of the skin phenotype of *Dgat2*^{-/-} mice resemble findings seen in essential fatty acid deficiency. Essential fatty acids are required for normal growth and skin function, and a deficiency in these fatty acids is characterized by growth retardation, skin abnormalities, and increased transepidermal water loss (31, 44, 45). In addition, linoleic acid is a component of acylceramide, a lipid thought to be involved in epidermal permeability barrier function (32). Analysis of the triglyceride fatty acid composition of liver and skin revealed that there were almost no essential fatty acids in triglycerides from *Dgat2*^{-/-} mice. Thus, DGAT2 appears to be specifically required to generate and maintain a pool of triglycerides containing essential fatty acids. Because DGAT2 is expressed in the neonatal epidermis, the barrier abnormality might be because of the absence of DGAT2 in this tissue. However, skin transplantation studies suggest that the barrier abnormality relates to the systemic lack of DGAT2, rather than DGAT2 deficiency in the epidermis itself. An alternative explanation is that DGAT2 expressed in other tissues can generate circulating lipids that correct the epidermal functional and structural defects.

Because the tissue expression pattern of DGAT2 in mice is similar to that observed in humans (7), it is likely that DGAT2 plays a similarly prominent role in triglyceride metabolism in humans. In humans, *DGAT2* is located at chromosome 11q13.3, and there are no obvious disorders with a phenotype similar to

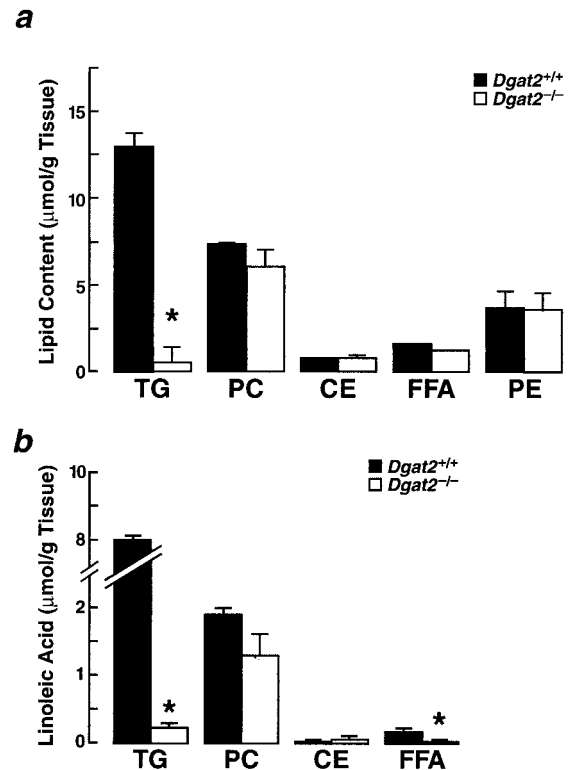


FIG. 12. Reduced triglyceride and linoleic acid content in skin from *Dgat2*^{-/-} mice. *a*, reduced triglyceride (TG) content in skin. Lipids were extracted from skin homogenates of three newborn mice of each genotype and analyzed by TLC. *, $p < 0.001$. *b*, reduced linoleic acid content in skin lipids. Lipids were extracted, and the linoleic acid content of each class was measured by gas-liquid chromatography. $n = 3$ /genotype. *, $p < 0.005$. **, $p < 0.05$. PC, phosphatidylcholine; CE, cholesterol esters; FFA, free fatty acids.

Dgat2^{-/-} mice that map to this locus. Interestingly, a recent human study found that decreased DGAT2 expression is a characteristic of psoriatic skin (46). In humans, the inhibition of DGAT enzymes and triglyceride synthesis is a potential pharmaceutical strategy to treat obesity and diabetes mellitus. DGAT1 inhibition is a promising target, because DGAT1-deficient mice have increased energy expenditure (18) and enhanced sensitivity to insulin and leptin (19, 20). The current study suggests that inhibition of DGAT2 should be approached cautiously because DGAT2 function appears to be crucial for survival.

Acknowledgments—We thank Q. Walker and B. Tow for blastocyst injections; S. Cases and P. Zhou for DGAT1 and DGAT2 expression vectors; B. Taylor for manuscript preparation; M. Shih for providing samples of placenta, yolk sac, and embryo RNA; L. Arnaboldi for as-

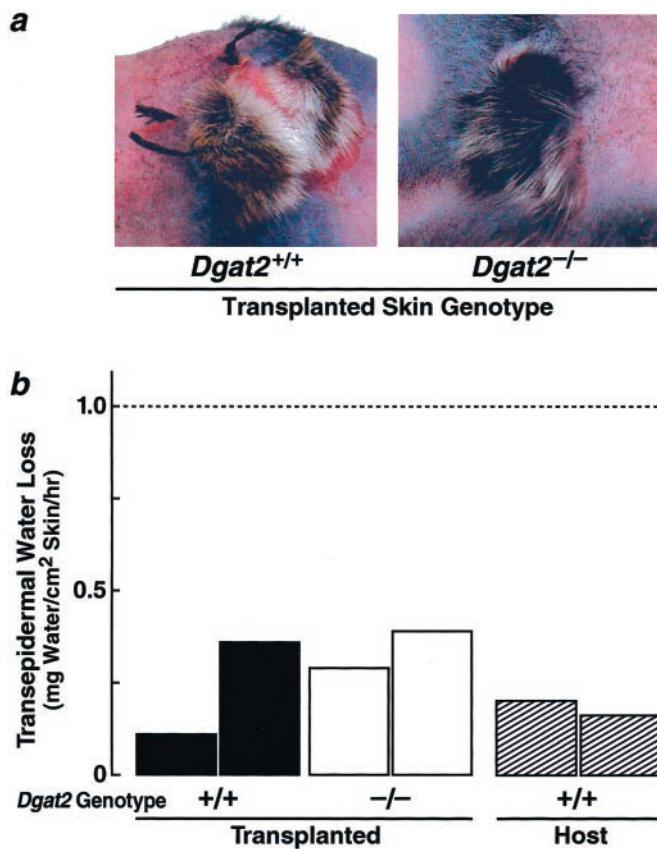


FIG. 13. Normal hair growth and transepidermal water loss in grafts of skin from *Dgat2*^{-/-} mice. *a*, normal hair growth in grafts 3 weeks after wild-type and *Dgat2*^{-/-} skin was transplanted onto the backs of athymic nude mice. Similar results were observed for four transplant experiments. *b*, similar transepidermal water loss in wild-type and *Dgat2*^{-/-} skin grafts and in skin of host nude mice, indicating that *Dgat2*^{-/-} skin grafts had a functional permeability barrier. The dashed line indicates a transepidermal water loss of 1 mg/cm²/h, which would be indicative of a defective permeability barrier with the electrolytic water analyzer used for this experiment.

sistance with lipid analysis; J. Fish for assistance with histology; C. Stoddart and J. Rivera for assistance with skin transplantation experiments; S. Ordway and G. Howard for editorial assistance; J. Carroll for graphics assistance; and J. Herz, H. Chen, R. Mahley, E. Yen, and C. Villanueva for comments on the manuscript.

REFERENCES

- Unger, R. H., and Zhou, Y. T. (2001) *Diabetes* **50**, Suppl. 1, S118-S121
- Unger, R. H., and Orci, L. (2002) *Biochim. Biophys. Acta* **1585**, 202-212
- Bell, R. M., and Coleman, R. A. (1980) *Annu. Rev. Biochem.* **49**, 459-487
- Brindley, D. N. (1991) in *Biochemistry of Lipids, Lipoproteins and Membranes* (Vance, D. E., and Vance, J. E., eds) pp. 171-203, Elsevier, Amsterdam
- Gunstone, F. D., Harwood, J. L., and Padley, F. B. (1994) *The Lipid Handbook*, 2nd Ed., pp. 646-651, Chapman & Hall, London
- Cases, S., Smith, S. J., Zheng, Y.-W., Myers, H. M., Lear, S. R., Sande, E., Novak, S., Collins, C., Welch, C. B., Lusis, A. J., Erickson, S. K., and Farese, R. V., Jr. (1998) *Proc. Natl. Acad. Sci. U. S. A.* **95**, 13018-13023
- Cases, S., Stone, S. J., Zhou, P., Yen, E., Tow, B., Lardizabal, K. D., Voelker, T., and Farese, R. V., Jr. (2001) *J. Biol. Chem.* **276**, 38870-38876
- Yen, C.-L. E., Stone, S. J., Cases, S., Zhou, P., and Farese, R. V., Jr. (2002) *Proc. Natl. Acad. Sci. U. S. A.* **99**, 8512-8517
- Yen, C.-L. E., and Farese, R. V., Jr. (2003) *J. Biol. Chem.* **278**, 18532-18537
- Cao, J., Lockwood, J., Burn, P., and Shi, Y. (2003) *J. Biol. Chem.* **278**, 13860-13866
- Cheng, D., Nelson, T. C., Chen, J., Walker, S. G., Wardwell-Swanson, J., Meegalla, R., Taub, R., Billheimer, J. T., Ramaker, M., and Feder, J. N. (2003) *J. Biol. Chem.* **278**, 13611-13614
- Cao, J., Burn, P., and Shi, Y. (2003) *J. Biol. Chem.* **278**, 25657-25663
- Lockwood, J. F., Cao, J., Burn, P., and Shi, Y. (2003) *Am. J. Physiol. Endocrinol. Metab.* **285**, E927-E937
- Oelkers, P., Cromley, D., Padamsee, M., Billheimer, J. T., and Sturley, S. L. (2002) *J. Biol. Chem.* **277**, 8877-8881
- Sorger, D., and Daum, G. (2002) *J. Bacteriol.* **184**, 519-524
- Sandager, L., Gustavsson, M. H., Stahl, U., Dahlqvist, A., Wiberg, E., Banas, A., Lenman, M., Ronne, H., and Stymne, S. (2002) *J. Biol. Chem.* **277**, 6478-6482
- Zhang, Q., Chieu, H. K., Low, C. P., Zhang, S., Heng, C. K., and Yang, H. (2003) *J. Biol. Chem.* **278**, 47145-47155
- Smith, S. J., Cases, S., Jensen, D. R., Chen, H. C., Sande, E., Tow, B., Sanan, D. A., Raber, J., Eckel, R. H., and Farese, R. V., Jr. (2000) *Nat. Genet.* **25**, 87-90
- Chen, H. C., Smith, S. J., Ladha, Z., Jensen, D. R., Ferreira, L. D., Pulawa, L. K., McGuire, J. G., Pitas, R. E., Eckel, R. H., and Farese, R. V., Jr. (2002) *J. Clin. Invest.* **109**, 1049-1055
- Chen, H. C., Ladha, Z., and Farese, R. V., Jr. (2002) *Endocrinology* **143**, 2893-2898
- Meyers, E. N., Lewandoski, M., and Martin, G. R. (1998) *Nat. Genet.* **18**, 136-141
- Snyder, F., and Stephens, N. A. (1959) *Biochim. Biophys. Acta* **34**, 244-245
- Folch, J., Lees, M., and Stanley, G. H. S. (1957) *J. Biol. Chem.* **226**, 497-509
- Watkins, S. M., Lin, T. Y., Davis, R. M., Ching, J. R., DePeters, E. J., Halpern, G. M., Walzem, R. L., and German, J. B. (2001) *Lipids* **36**, 247-254
- Bligh, E. G., and Dyer, W. J. (1959) *Can. J. Biochem. Physiol.* **37**, 911-917
- Holleran, W. M., Man, M. Q., Gao, W. N., Menon, G. K., Elias, P. M., and Feingold, K. R. (1991) *J. Clin. Invest.* **88**, 1338-1345
- Madison, K. C., Swartzendruber, D. C., Wertz, P. W., and Downing, D. T. (1987) *J. Invest. Dermatol.* **88**, 714-718
- Hou, S. Y., Mitra, A. K., White, S. H., Menon, G. K., Ghadially, R., and Elias, P. M. (1991) *J. Invest. Dermatol.* **96**, 215-223
- Grubauer, G., Elias, P. M., and Feingold, K. R. (1989) *J. Lipid Res.* **30**, 323-333
- Holt, R. I. (2002) *Trends Endocrinol. Metab.* **13**, 392-397
- Elias, P. M., and Brown, B. E. (1978) *Lab. Invest.* **39**, 574-583
- Elias, P. M., Brown, B. E., and Ziboh, V. A. (1980) *J. Invest. Dermatol.* **74**, 230-233
- Kuramoto, N., Takizawa, T., Matsuki, M., Morioka, H., Robinson, J. M., and Yamanishi, K. (2002) *J. Clin. Invest.* **109**, 243-250
- Chen, H. C., Smith, S. J., Tow, B., Elias, P. M., and Farese, R. V., Jr. (2002) *J. Clin. Invest.* **109**, 175-181
- Wertz, P. W., and Downing, D. T. (1990) *J. Lipid Res.* **31**, 1839-1844
- Chen, H. C., Stone, S. J., Zhou, P., Buhman, K. K., and Farese, R. V., Jr. (2002) *Diabetes* **51**, 3189-3195
- Chen, H. C., Jensen, D. R., Myers, H. M., Eckel, R. H., and Farese, R. V., Jr. (2003) *J. Clin. Invest.* **111**, 1715-1722
- Wang, N. D., Finegold, M. J., Bradley, A., Ou, C. N., Abdelsayed, S. V., Wilde, M. D., Taylor, L. R., Wilson, D. R., and Darlington, G. J. (1995) *Science* **269**, 1108-1112
- Moitra, J., Mason, M. M., Olive, M., Krylov, D., Gavrilova, O., Marcus-Samuels, B., Feigenbaum, L., Lee, E., Aoyama, T., Eckhaus, M., Reitman, M. L., and Vinson, C. (1998) *Genes Dev.* **12**, 3168-3181
- Shimomura, I., Hammer, R. E., Richardson, J. A., Ikemoto, S., Bashmakov, Y., Goldstein, J. L., and Brown, M. S. (1998) *Genes Dev.* **12**, 3182-3194
- Farese, R. V., Jr., Ruland, S. L., Flynn, L. M., Stokowski, R. P., and Young, S. G. (1995) *Proc. Natl. Acad. Sci. U. S. A.* **92**, 1774-1778
- Raabe, M., Flynn, L. M., Zlot, C. H., Wong, J. S., Véniant, M. M., Hamilton, R. L., and Young, S. G. (1998) *Proc. Natl. Acad. Sci. U. S. A.* **95**, 8686-8691
- Farese, R. V., Jr., Cases, S., Ruland, S. L., Kayden, H. J., Wong, J. S., Young, S. G., and Hamilton, R. L. (1996) *J. Lipid Res.* **37**, 347-360
- Burr, G. O., and Burr, M. M. (1929) *J. Biol. Chem.* **82**, 345-367
- Cartlidge, P. (2000) *Semin. Neonatol.* **5**, 273-280
- Wakimoto, K., Chiba, H., Michibata, H., Seishima, M., Kawasaki, S., Okubo, K., Mitsui, H., Torii, H., and Imai, Y. (2003) *Biochem. Biophys. Res. Commun.* **310**, 296-302